ACI STRUCTURAL JOURNAL TECHNICAL PAPER

Title no. 96-S95

Strengthening Reinforced Concrete Beams Using Fiber Reinforced Polymer (FRP) Laminates

by N. F. Grace, G. A. Sayed, A. K. Soliman and K. R. Saleh

The behavior of reinforced concrete beams strengthened with various types of fiber reinforced polymer (FRP) laminates is presented in this paper. The experimental program included strengthening and testing 14 simply supported rectangular cross section beams. Each beam was initially loaded above its cracking load. The cracked beams were strengthened with FRP laminates and then tested until complete failure. Five available strengthening systems of various types of carbon/glass fiber reinforced polymer (CFRP/GFRP) strengthening materials were used. These materials included two types of CFRP sheets, bi- and unidirectional GFRP sheets, and CFRP plates. The effects of strengthening on deflection, failure load and failure mode, strain, and beam ductility are discussed. In addition, the influence of different numbers of FRP layers, type of epoxy, and strengthening pattern on the behavior of beams was examined. The ratio of absorbed energy at failure to total energy, or energy ratio, was used as a measure of beam ductility.

It is concluded that, in addition to the longitudinal layers, the fibers oriented in the vertical direction forming a U-shape around the beam cross section significantly reduce beam deflections and increase beam load carrying capacity. Furthermore, the presence of vertical FRP sheets along the entire span length eliminates the potential for rupture of the longitudinal sheets. The combination of vertical and horizontal sheets, together with a proper epoxy, can lead to a doubling of the ultimate load carrying capacity of the beam. However, all the strengthened beams experienced brittle failure, mandating a higher factor of safety in design.

Keywords: ductility; reinforced concrete; strengthening.

INTRODUCTION

The urgent need to strengthen concrete structures is on the rise. Various motivations lead to the increased demand for strengthening. Deterioration and aging of concrete structures are not the only reasons for strengthening beams. Other reasons include upgrading design standards, committing mistakes in design or construction, exposure to unpredicted loads such as truck hits or powerful earthquakes, and changing the usage of the structure. Moreover, the ever-increasing truck loads are sometimes beyond the design loads of most bridges in North America that were built after World War II. Since then, the average service loads were increased by 40 percent.[1] The strengthening should ideally minimize the amount of material added to the structure to avoid increasing the dead load or decreasing the clearance requirements. Along with that, strengthening should minimize disruption to the structure and its usage. Bonding steel plates might be considered as a very convenient method for strengthening indoor beams. However, the main disadvantage of using steel plates for outdoor applications is corrosion of steel. This corrosion is serious not because it reduces the plates' strength, but because it destroys the bonding between the plates and the epoxy.

The use of fiber reinforced polymers (FRP) as strengthening materials has been gaining the interest of many researchers for the last two decades. These materials are superior to steel when it comes to comparing the resistance to electrochemical corrosion, strength to weight ratio, ease of handling, fatigue resistance, and availability in any length or shape. The successful use of FRP in aerospace, sports, recreation, and automobile industries helped in decreasing FRP cost. This decrease in cost, combined with the savings due to the elimination of future maintenance and repair costs, makes the application of FRP economically competitive with their steel counterparts.

In 1991, Saadatmanesh and Ehsani studied the strengthening of beams using GFRP plates;[2] they concluded that bonding GFRP plates to the concrete reduced the crack size at all load levels. It was also indicated that using GFRP plates reduced the ductility of the beams. In 1994, Alfarabi et al.[3] tested concrete beams strengthened using different patterns of GFRP plates; they recommended the use of I-jackets to eliminate plate separation and diagonal tension failure and to avoid a significant decrease in ductility. In another study,[4] they examined the feasibility of using different shapes of GFRP plates for shear strengthening; plates, wings, and I-jacket patterns were tested. It was concluded that only the I-jacket shape converted the mode of failure to flexural mode. The local shear failure of concrete beams strengthened with CFRP plates was studied recently by Saadatmanesh et al.[5] and He.[6] This failure occurs in the concrete between the FRP plate and the steel reinforcement. Such failure was attributed to the shear and normal stress concentration at the plate ends and around the flexural cracks. Takahashi et al.[7] examined the use of U-jacket CFRP sheets and concluded that this pattern of strengthening is able to control the progress of peeling and shift the mode of failure from peeling to rupture of sheets. Swamy et al.[8] studied the ductility of beams strengthened with FRP plates. It was concluded that the ductility of these beams can be improved using innovative design techniques that minimize the relative bond slip between the plates and the beam.

RESEARCH SIGNIFICANCE

This research work addresses two major concerns. The first is to examine the effect of using available FRP strengthening systems with different patterns in strengthening reinforced concrete beams. The second is to evaluate the ductility of FRP strengthened beams. The findings of this research can contribute to the development of design recommendations and guidelines currently undertaken by ACI Committee 440.

ACI Structural Journal, V. 96, No. 5, September-October 1999.
Received May 12, 1998, and reviewed under Institute publication policies. Pertinent discussion will be published in the July-August 2000 *ACI Structural Journal* if received by March 1, 2000.

ACI member **N. F. Grace** *is a professor in the Department of Civil Engineering at Lawrence Technological University, Southfield, Mich. His reserarch interests include the application of advanced concrete materials in reinforced and prestressed concrete structures.*

G. A. Sayed *is a professor emeritus in civil and environmental engineering at the University of Windsor, Windsor, Ontario, Canada.*

A. K. Soliman *is a professor in the Department of Civil Engineering at Suez Canal University, Port-Said, Egypt.*

K. R. Saleh *is a PhD candidate in the Department of Civil Engineering at Lawrence*

EXPERIMENTAL WORK

The experimental work consisted of testing 14 simply supported beams. All beams had the same dimensions and flexural and shear reinforcements. The beams had a rectangular cross section with a 152-mm (6-in.) width, 292-mm (11.5-in.) height, and a clear span of 2743 mm (9 ft). Two 16-mm (No. 5) steel bars were used for flexural reinforcement at the bottom and top of each beam. Steel stirrups of 8 mm (No. 3) were spaced every 152 mm (6 in.) for shear reinforcement. First, each beam was cracked by applying a midspan load of 44.8 kN (10 kips). After cracking, each beam was strengthened with a FRP material. The beams were then tested with a concentrated load applied at midspan until complete failure took place. Five FRP strengthening systems were used in this research project. These systems consisted of two types of CFRP sheets (Systems I and II), two types of GFRP sheets (Systems III and IV), and CFRP plates (System V). Four types of epoxies, identified as Types 1-4, were used in these systems. Table 1 shows the combinations of strengthening materials and epoxies for the available strengthening systems. The available mechanical properties of the strengthening materials and epoxies are shown in Tables 2 and 3, respectively.

Table 1—Fiber reinforced polymer strengthening systems

Strengthening system	I	II	III	IV	V
Type of strengthening material	CFRP*	CFRP*	GFRP*	GFRP*	CFRP†
Epoxy type	1	2	2	3	4

*Sheets.
†Plates.

Table 2—Properties of strengthening laminates

Strengthening system	I	II	III	IV		V
Type of fibers	CFRP	CFRP	GFRP	GFRP		CFRP
Fibers orientation	Unidirectional	Unidirectional	Unidirectional	Bidirectional		Unidirectional
				x-direction	y-direction	
Tensile strength, MPa (ksi)	2937 (426)	758 (110)	413 (60)	482 (70)	310 (45)	2399 (348)
Modulus of elasticity, GPa ($\times 10^3$ ksi)	230 (33.4)	62 (9.0)	21 (3.0)	14 (2.1)	11 (1.6)	149 (21.7)
Failure strain, percent	1.2	1.2	2.0	3.0		1.4
Thickness, mm ($\times 10^{-1}$), in.	5 (0.02)	13 (0.05)	10 (0.04)	13 (0.05)		13 (0.05)

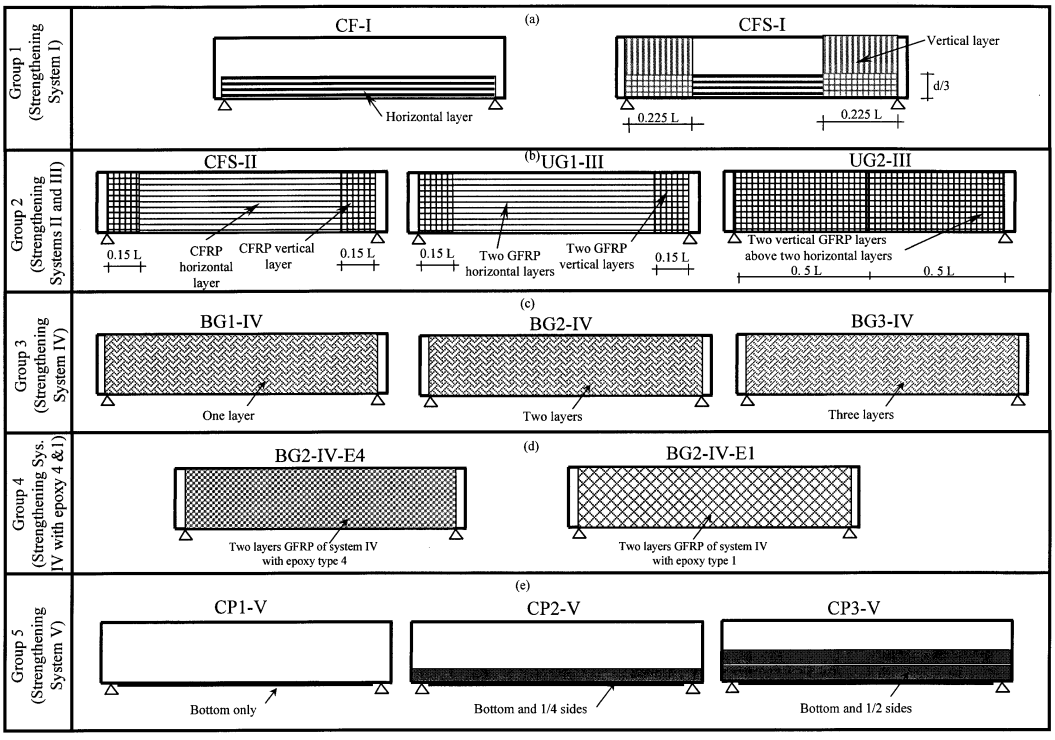

Fig. 1—Arrangements of strengthening of tested beams.

Technological University.

In addition, a control beam (CONT) was tested to determine its behavior, ductility, and load-carrying capacity. The tested beams were divided into five groups (in addition to the control beam). Table 4 explains the nomenclature of the tested beams and the groups, while Fig. 1 shows the patterns of the strengthening materials. The reinforcement ratios of the tested beams, including the strengthening materials, are also shown in Table 4.

Beams CF-I and CFS-I [Fig. 1(a)] were strengthened with strengthening System I using epoxy Type 1. Beam CF-I was strengthened for flexural only; CFRP sheets oriented in the horizontal direction were applied to the bottom of the beam and extended along the sides to 1/3 of the total depth of the beam. Beam CFS-I was strengthened for both flexural and shear. CFRP sheets with fibers oriented in the horizontal direction were applied in a fashion similar to that of the first beam. CFRP sheets with fibers oriented in the vertical direction were applied at the ends of the beam, forming a U-shape around the beam cross section. The vertical sheets occupied 0.225 of the span length at each end. They were attached to the horizontal sheets.

Beams CFS-II, UG1-III, and UG2-III are shown in Fig. 1(b). Beam CFS-II was strengthened with strengthening System II that consisted of CFRP sheets and Epoxy 2. A U-shaped layer with the fibers oriented in the longitudinal direction covered the bottom and both sides of the beam for the entire span. In addition, a U-shaped layer, with the fibers aligned in the vertical direction, was attached to the first layer and covered 0.15 of the span at each support. Beam UG1-III was strengthened with strengthening System III in a pattern similar to that of Beam CFS-II, except that every CFRP layer was replaced with two GFRP layers. Beam UG2-III was strengthened with strengthening System III in a manner similar to that of beam UG1-III, except that each vertical layers was extended to cover half of the span. It should be noticed that epoxy Type 2 was used in both of Systems II and III.

Beams BG1-IV, BG2-IV, and BG3-IV are shown in Fig. 1(c). These beams were strengthened with strengthening System IV that consisted of bidirectional (45/-45 deg) GFRP sheets and epoxy Type 3. One, two, and three layers were epoxied to Beams BG1-IV, BG2-IV, and BG3-IV, respectively. The GFRP strengthening sheets were applied to the bottom and sides of the beams for the entire span length. Each layer was applied independently, with additional layers applied after the previous layer had cured.

Beams BG2-IV-E4 and BG2-IV-E1 are shown in Fig. 1(d). These two beams were strengthened with combination of two layers of bidirectional (45/-45 deg) GFRP sheets of System IV but using epoxy Types 4 and 1, respectively. Their strengthening patterns were similar to Beam BG2-IV.

Beams CP1-V, CP2-V, and CP3-V are shown in Fig. 1(e). These beams were strengthened with strengthening System V, which consisted of CFRP plates and epoxy Type 4. Two plates 80-mm (3.1-in.) wide were placed side by side to the bottom of Beam CP1-V along its full clear span. Beam CP2-V was strengthened in the same manner as Beam CP1-V, with additional plates placed on both sides for 1/4 of the depth of the cross section. One 80-mm-(3.1-in.)-wide plate was placed on each side for the length of the beam. Beam CP3-V was strengthened in the same manner as Beam CP2-V, except that one additional 50-mm-(2.0-in.)-wide plate was attached to each side above the 80-mm (3.1-in.) plate. The fibers of all plates were oriented in the longitudinal direction of the beams.

Concrete with a compressive strength of 48.26 MPa (7000 psi) and typical slump of 200 mm (8 in.) was provided by a local supplier. High-strength steel [650 MPa (94 ksi) tensile strength] was used for reinforcement. Each beam was instrumented with strain gages, dial gages, potentiometers, and one load cell.

Table 3—Properties of epoxy

Epoxy type	1	2	3	4
Tensile strength, MPa (psi)	29.8 (4251)	66.5 (9500)	95.0 (13,800)	24.8 (3571)
Modulus of elasticity, GPa (ksi)	—	2.7 (400)	3.7 (540)	4.5 (650)
Elongation at break, percent	—	5.0	4.6	1.0
Shear strength, MPa, (psi)	9.8 (1391)	—	—	24.8 (3571)
Flexural strength, MPa (psi)	39.2 (5700)	79.0 (11,500)	152 (22,000)	46.8 (6771)

Table 4—Details of tested beams

Group	Beam	Strengthening system	Epoxy type	$\rho^* \times 10^{-2}$	Remarks
1	CF-I	I	1	1.32	Strengthening for flexural only
	CFS-I			1.32	Strengthening for flexural and shear
2	CFS-II	II	2	1.76	One Hl† layer and 2 Vl‡ layers of 0.15L§ length
	UG1-III	III		2.42	Two Hl layers and 2 Vl layers of 0.15L§ length
	UG2-III			2.42	Two Hl layers and 2 Vl layers of 0.5L§ length
3	BG1-IV	IV	3	1.51	One layer
	BG2-IV			1.92	Two layers
	BG3-IV			2.35	Three layers
4	BG2-IV-E4	Combination‖	4	1.52	GFRP sheets of System IV with epoxy Type 4
	BG2-IV-E1		1	1.52	GFRP sheets of System IV with epoxy Type 1
5	CP1-V	V	4	1.65	Strengthening bottom only
	CP2-V			2.19	Strengthening bottom and 1/4 sides
	CP3-V			2.56	Strengthening bottom and 1/2 sides

*Equivalent reinforcement ratio at midsection (contribution of strengthening material above neutral axis ignored).
†Longitudinal fibers along span.
‡Vertical U-shape fibers.
§Clear span.
‖Combination of GFRP sheets of System IV with epoxies Type 4 or 1.
Notes: I-V = strengthening system; C = CFRP; G = GFRP; F = flexural strengthening; S = shear strengthening; B = bidirectional; U = unidirectional; P = plates; and E = epoxy.

RESULTS

Deflections

Table 5 shows the midspan deflections of all the beams at their failure loads. The largest deflection was experienced by Beam BG2-IV-E4. This beam had a maximum deflection of 139 mm (5.5 in.), twice that of the control beam's 63 mm (2.51 in.). Conversely, Beams BG1-IV and CFS-I experienced the lowest deflections of 72 and 74 mm (2.85 and 2.91 in.) at ultimate load, respectively. All the strengthened beams experienced deflections larger than those of the control beam at their failure loads. In addition, all the strengthened beams had failure loads higher than that of the control beam. For comparison, the deflections of the beams at the yield load of the control beam of 66.7 kN (15 kips) are also shown in Table 5. The table shows that using FRP strengthening materials significantly reduces deflections when compared at yield load. This decrease in deflection was dependent on the type of strengthening material, the epoxy used, and the strengthening pattern. The smallest deflections of 14 mm (0.54 in.) were only 55 percent of that of the control beam and were experienced by Beams UG2-III and CP3-V. However, the amount of strengthening material and the required preparation time for strengthening Beam UG2-III were almost twice that required for Beam CP3-V.

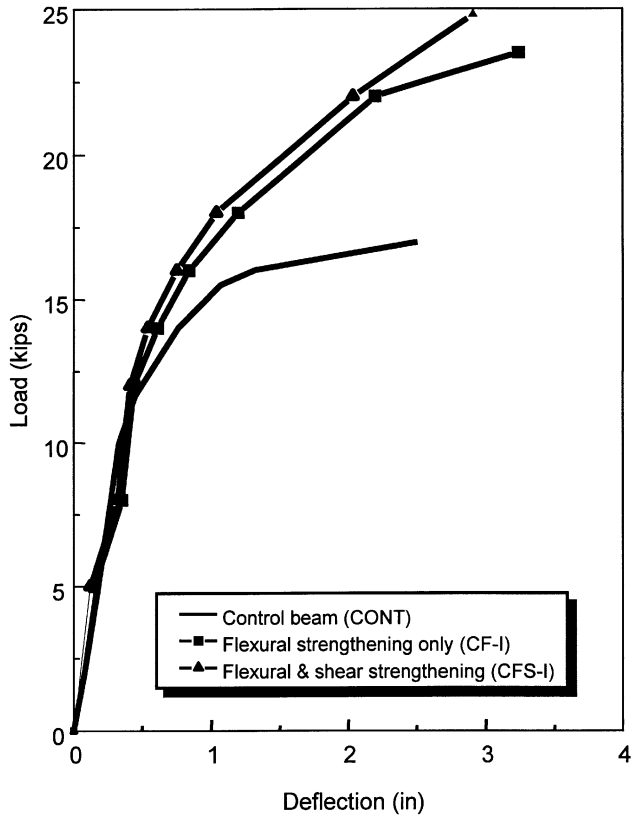

Fig. 2—Response of Group 1 strengthened beams.

In Fig. 2, the load-deflection relationships of the control Beam CONT and the two strengthened Beams CF-I and CFS-I are compared. At a load of 66.7 kN (15 kips), flexural strengthening of Beam CF-I decreased its deflection by 24 percent, while a combination of both flexural and shear strengthening in beam CFS-I decreased its deflection by 48 percent. These large reductions in deflection are noticeable at a high load level (above 70 percent of the load carrying capacity of the beams). This indicates that while strengthening the maximum shear areas does not significantly decrease deflections at service loads, it does reduce deflections by 1/2 at higher load levels. This was expected since the presence of the vertical CFRP sheets at both ends of the beam eliminated the development of diagonal tension cracks.

Fig. 3 shows the load-deflection relationships for Beams CFS-II, UG1-III, and UG2-III, as well as the control beam. As shown, the behavior of the three strengthened beams was identical up to a load of 72 kN (16 kips). Afterwards, the deflection of Beam UG1-III was larger than that of Beam UG2-III because of the effect of the extended vertical layers that limited the cracking of concrete. The deflection of Beam UG1-III was larger than that of Beam CFS-II, because the modulus of elasticity of the CFRP sheets is three times that of the GFRP sheets (Table 2).

Fig. 4 shows the load-deflection relationships of the control beam and the Beams BG1-IV, BG2-IV, and BG3-IV. As shown in Fig. 4 and Table 5, Beams BG1-IV, BG2-IV, and BG3-IV experienced deflections of 72, 96, and 104 mm (2.85, 3.80, and 4.10 in.), respectively. Beam BG1-IV had the lowest deflection of the tested beams. However, at a load of 66.7 kN (15 kips), its deflection was second highest. This can be explained by the low failure load of this beam (only a 6 percent increase over the control beam). The behavior of Beams BG2-IV and BG3-IV was similar, with the exception of their residual deflection. While Beam BG2-IV experienced 38-mm (1.5-in.) residual deflection, Beam BG3-IV experienced only 25-mm (1.-in). Aside from the effect on residual deflection, no significant effect of the number of layers on deflection was noticed. At the start of delamination

Table 5—Comparison between failure loads and deflections

Group	Beam	Failure load		Deflection at 15 kips		Maximum deflection	
		kN (kips)	Ratio to CONT	mm (in.)	Ratio to CONT	mm (in.)	Ratio to CONT
1	CF-I	104.5 (23.5)	1.38	19 (0.74)	0.75	82 (3.24)	1.29
	CFS-I	110.3 (24.8)	1.46	13 (0.51)	0.76	74 (2.91)	1.15
2	CFS-II	108.9 (24.5)	1.44	13 (0.81)	0.83	91 (3.59)	1.43
	UG1-III	164.5 (37.0)	2.18	17 (0.67)	0.68	119 (4.68)	1.86
	UG2-III	177.9 (40.0)	2.35	14 (0.55)	0.56	82 (3.24)	1.29
3	BG1-IV	80.0 (18.0)	1.06	23 (0.90)	0.91	72 (2.85)	1.13
	BG2-IV	94.7 (21.3)	1.26	22 (0.86)	0.87	96 (3.80)	1.51
	BG3-IV	92.5 (20.8)	1.22	19 (0.76)	0.78	104 (4.10)	1.63
4	BG2-IV-E4	142.2 (32.0)	1.88	22 (0.87)	0.88	139 (5.50)	2.19
	BG2-IV-E1	129.0 (29.0)	1.70	24 (0.94)	0.96	114 (4.50)	1.79
5	CP1-V	110.3 (24.8)	1.46	22 (0.87)	0.88	81 (3.20)	1.27
	CP2-V	120.1 (27.0)	1.59	19 (0.76)	0.77	93 (3.67)	1.46
	CP3-V	131.2 (29.5)	1.73	14 (0.55)	0.56	109 (4.31)	1.71
CONT		75.2 (16.9)		25 (0.98)		64 (2.51)	

in Beams BG2-IV and BG3-IV, their deflections surged such that the load–deflection curve was flat until the beams were unloaded. Reloading the beams again yielded even higher deflections until complete delamination took place.

Fig. 5 shows the load-deflection relationships of Beams BG2-IV-E4 and BG2-IV-E1 compared to those of BG2-IV. Using GFRP bidirectional sheets is the common factor between these three beams. Before a load of 72 kN (16 kips), the behaviors of Beams BG2-IV-E1 and BG2-IV-E4 were identical. After a load of 72 kN (16 kips), Beam BG2-IV-E4 experienced a larger deflection than BG2-IV-E1. To determine if the cause of this large difference in deflection was the epoxy or some other element in the testing procedure, the beam was unloaded and reloaded. The same deflection values were recorded since the only difference between BG2-IV-E4 and BG2-IV-E1 was in the use of epoxy type. These results show that the type of epoxy can significantly influence beam deflection. Table 3 shows that both the flexural and the tensile strength of Type I epoxy were higher than those of Type IV. Therefore, using a strong epoxy can reduce the deflection of a strengthened beam at high load. In addition, it shows that if the delamination problem is eliminated, which was experienced by Beams BG2-IV, the ultimate load capacity of the Beams BG2-IV-E4 and BG2-IV-E1 is significantly improved.

Fig. 6 shows the load-deflection relationships for Beams CP1-V, CP2-V, and CP3-V, as well as the control beam. Deflections at a load of 66.7 kN (15 kips) were 22, 19, 14, and 25 mm (0.87, 0.76, 0.57, and 0.98 in.), respectively. Differences in deflections among the three strengthened beams started just above the cracking load, where the CFRP plates are effective in increasing the stiffness of the beams. The high modulus of elasticity of the CFRP plates increased the reinforcing ratio of the beam. In addition, it can be seen that the beam strengthened with CFRP plates on the bottom and on half of its sides (Beam CP3-V) experienced the lowest deflection at the ultimate load, and its ultimate load carrying capacity increased significantly.

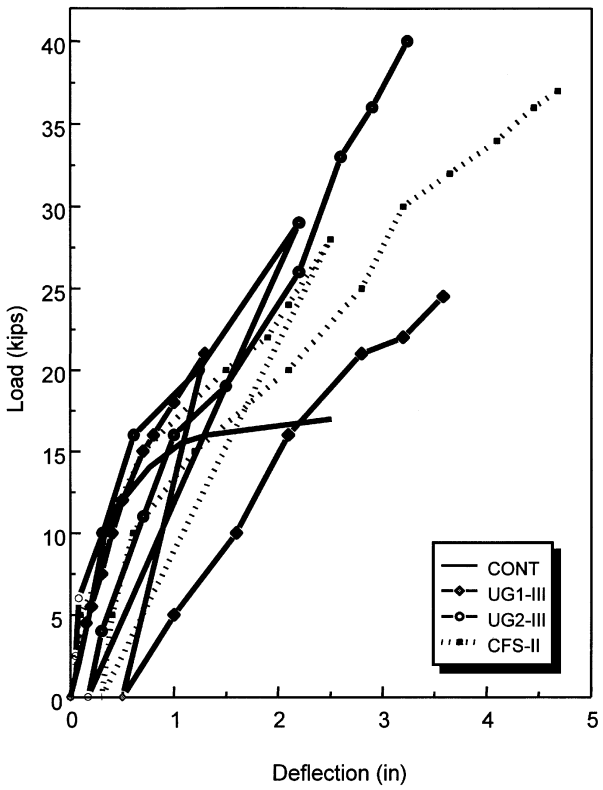

Fig. 3—Response of Group 2 strengthened beams.

FAILURE LOADS

Table 5 summarizes the maximum loads experienced by the tested beams. Beam UG2-III exhibited the maximum load carrying capacity, which is about 2.35 times that of the control beam. By comparing the load-deflection relationships for Beams CF-I and CFS-I, it is obvious that strengthening the beams with vertical U-shape layers at the ends improved the beams' load-carrying capacity (Fig. 2).

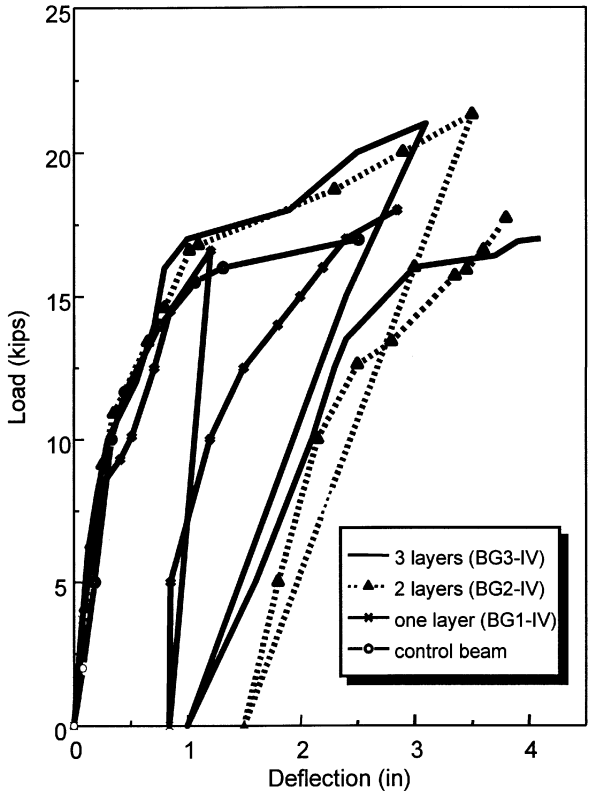

Fig. 4—Response of Group 3 strengthened beams.

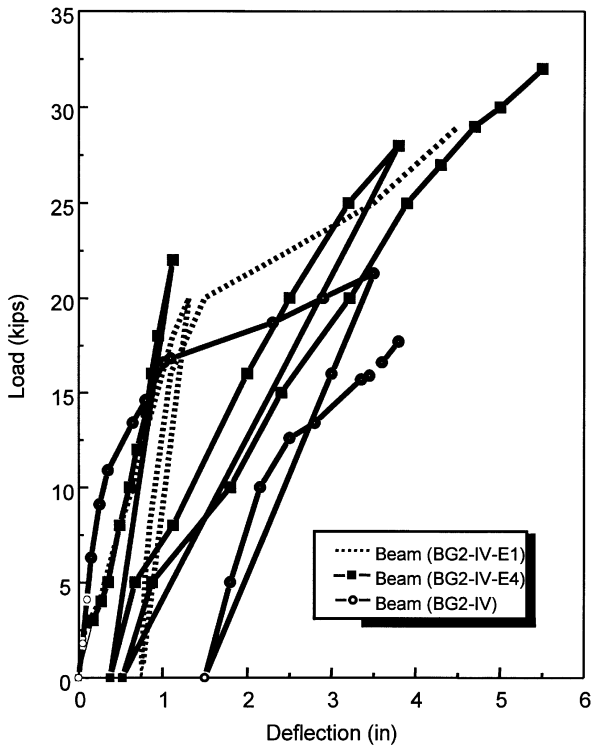

Fig. 5—Response of Group 4 strengthened beams.

Comparing the results of Beams UG2-III and CONT shows that the load-carrying capacity can be easily doubled if a beam is strengthened with both vertical and horizontal layers covering the entire span. Furthermore, comparing results of beams CFS-II and CFS-I indicates that both beams experienced the same load carrying capacity, suggesting that the CFRP sheets of strengthening Systems I and II may lead to the same results in beams strengthening (Table 5). However, as expected, the load carrying capacity of Beam UG2-III was higher than that of Beam UG1-III (Fig. 3).

Fig. 4 shows the load-maximum deflection relationships for Beams BG1-IV, BG2-IV, and BG3-IV, as well as the control beam. The beams failed at 80.0, 94.7, 92.5, and 75.2 kN (18.0, 21.3, 20.8, and 16.9 kips), respectively. Using one layer of GFRP increased the failure load from 75.2 kN (16.9 kips) in Beam CONT to 80.0 kN (18.0 kips) in Beam BG1-IV—only a 6 percent increase. Bonding another layer of GFRP onto Beam BG2-IV increased the failure load to 94.7 kN (21.3 kips), a 25.5 percent increase over the control beam and a 18.3 percent increase overBeam BG1-IV. However, adding a third layer of GFRP over the first two layers did not increase the failure load, as shown by the behavior of Beam BG3-IV. Failure of Beam BG1-IV occurred due to the rupture of GFRP sheets, followed by crushing of concrete. Using two layers of GFRP sheets in Beam BG2-IV cut the stresses in GFRP sheets in half and resulted in delamination between the two GFRP sheets and the concrete. Bonding a third layer of GFRP did not change the failure load as the overall load carrying capacity was governed mainly by the epoxy bond strength. In the same way, Beam BG3-IV also experienced a delamination failure similar to that of Beam BG2-IV. Therefore, to exploit the full strength of strengthening sheets, a minimum value of epoxy strength is needed. If the strength of the epoxy is less than this value, the overall load carrying capacity of the beam will be governed by delamination failure rather than sheets rupture. Therefore, the strength of epoxy, as well as the strength of the FRP sheets, are important in maximizing the strength of the beams. Comparing results of Beams CFS-I and BG1-IV shows that Beam CFS-I exhibited higher load carrying capacity, as shown in Table 5. This was expected due to the higher strength and modulus of elasticity of the CFRP sheets used in Beam CFS-I.

As shown in Fig. 5 and Table 5, the failure loads of Beams BG2-IV-E1, BG2-IV-E4, and BG2-IV were 129.0, 142.3, and 94.7 kN (29.0, 32.0, and 21.3 kips), respectively. Comparing results of Beams BG2-IV, BG2-IV-E4, and BG2-IV-E1 indicates that ultimate load-carrying capacity can be significantly improved by using the GFRP sheets of strengthening System IV with the proper epoxy, as given in Table 5. Comparing results of Beams CP1-V, CP2-V, and CP3-V shows that the addition of plates on both sides of the beam significantly increased the load carrying capacity of the beam (Table 5 and Fig. 6).

Strains

Fig. 7 shows the load-strain relationships for Beams CP1-V, CP2-V, and CP3-V, as well as that of the control beam. The results suggest that the presence of CFRP plates changed the distribution of compressive strain in concrete. In the unstrengthened beam, the stress in steel bars increases until the steel reaches its yield point. Thereafter, a large portion of any extra stress is absorbed by large deformations in the steel, which lowers the increase of concrete compressive strain. In strengthened beams, tensile stresses are shared between the steel bars and the strengthening plates, so the stresses carried by the steel bars will be less and may not reach the yield strength of steel. Therefore, concrete strains in the strengthened beams are higher than those in the control beam at the same load.

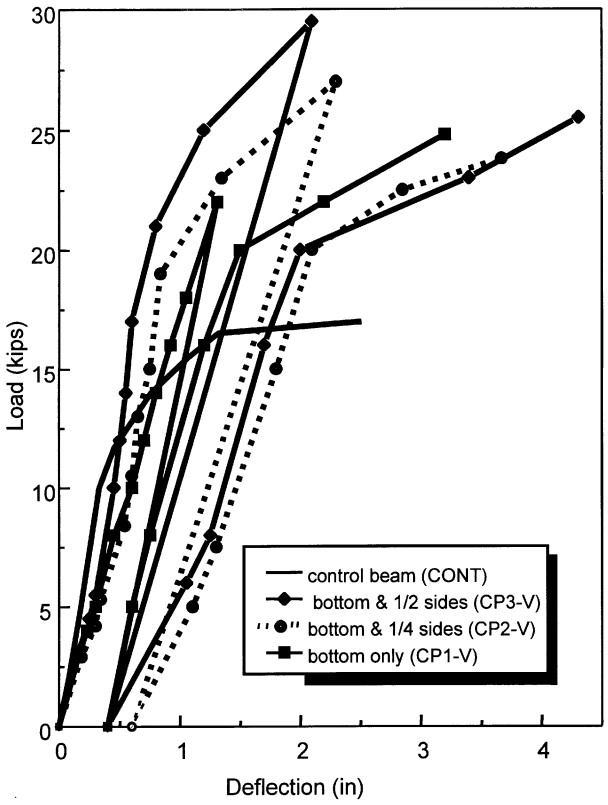

Fig. 6—Response of Group 5 strengthened beams.

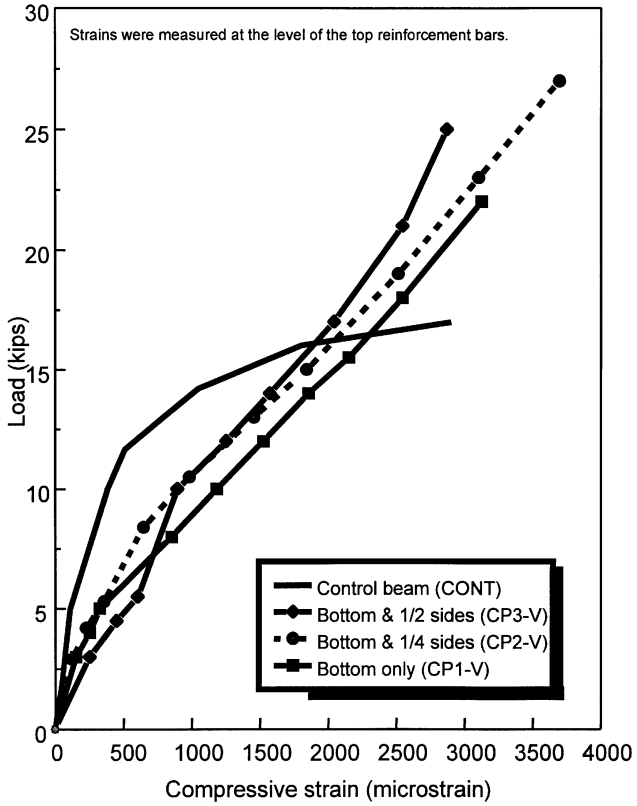

Fig. 7—Strain response of Group 5 beams during first cycle of

Failure modes and cracking patterns

Fig. 8 (a) through (m) show the failure modes of all the tested beams. Examination of these figures suggests that all beams experienced flexural failure, and all beams except Beam UG2-III failed in tension.

Fig. 8(a) and (b) show the failed sections of Beams CF-I and CFS-I, respectively. The presence of the vertical layers of CFRP sheets at the ends of Beam CFS-I limited the propagation of cracks to the unstrengthened area of the beam. Therefore, all the diagonal cracks ended at the intersection of the horizontal and the vertical sheets. Removing the strengthening sheets after failure and inspecting the beams revealed that diagonal cracks did not extend beneath the vertical sheets. However, the diagonal cracks were well-distributed along the span of Beam CF-I and extended

(a)

(b)

(c)

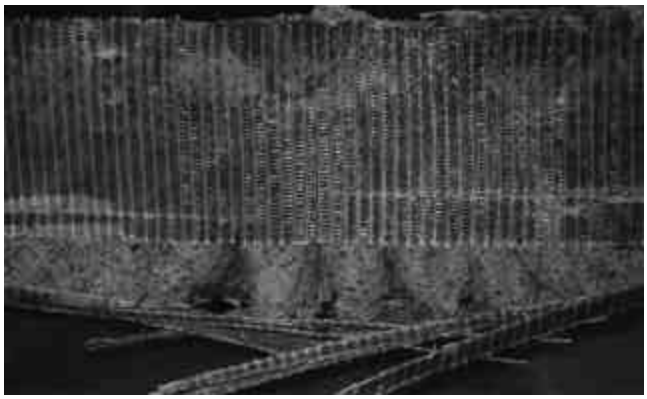

(d)

(e)

(f)

(g)

Fig. 8—Failed sections of beams: (a) CF-I; (b) CFS-I; (c) CFS-II; (d) UG1-III; (e) UG2-III; (f) BG1-IV; and (g) BG2-IV.

beneath the horizontal sheets. Thereupon, the use of vertical sheets is essential so that the growth of diagonal cracks will be limited.

Fig. 8(c), (d), and (e) show the failed section of Beams CFS-II, UG1-III, and UG2-III, respectively. Beams UG1-III and UG2-III had the same reinforcing ratio at their midsections; however, their flexural modes of failure were quite different. Beam UG2-III failed in a compressive mode by crushing of concrete, while Beam UG1-III failed in a tensile mode by rupture in the GFRP sheets. Calculations show that the midsection of Beam UG2-III was under-reinforced (less than the balanced ratio). Evidently, the fact that the concrete was strengthened by the two vertical layers affected the mode of failure. Rupture lines experienced in the GFRP sheets on both sides of Beam UG1-III, but were present only in the span between the two vertical layers. By eliminating the span in between the two vertical layers, as in Beam UG2-III, these rupture lines were eliminated. The failure of Beam CFS-II was very similar to the failure of Beam UG1-III, in which rupture occurred in the GFRP sheets at midspan.

The failed sections of Beams BG1-IV, BG2-IV, and BG3-IV are shown in Fig. 8(f), (g), and (h), respectively. As shown in Fig. 8(c), Beam BG1-IV failed by rupture of the GFRP sheets. However, in Beams BG2-IV and BG3-IV neither the concrete nor the strengthening sheets failed. The failure of Beams BG2-IV and BG3-IV was the result of delamination between the GFRP sheets and concrete, caused by the failure of the bonding epoxy between the concrete and the strengthening sheets. After failure, the strengthening sheets were removed to examine the cracking pat-

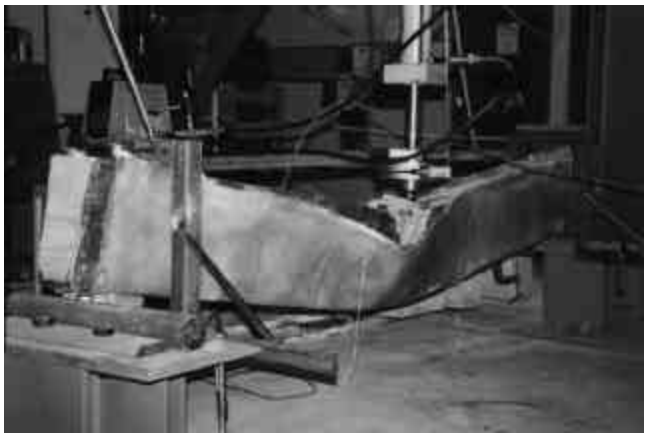

(h)

(i)

(j)

(k)

(l)

(m)

Fig. 8 (cont.)—Failed sections of beams: (h) BG3-IV; (i) BG2-IV-E4; (j) BG2-IV-E1; (k) CP1-V; (l) CP2-V; and (m) CP3-V.

tern. One large crack was developed at the midspan of Beam BG1-IV, and the total number of cracks in Beam BG1-IV was less than that of Beams CF-I and CFS-I. This is expected, since Beam BG1-IV was strengthened over the entire depth of the beam, whereas in Beams CF-I and CFS-I, the horizontal CFRP sheets were not applied over the entire depth. Obviously, applying the strengthening material in a U-shape over the depth of the beam is effective in limiting the growth of cracks.

Fig. 8(i) and (j) show the failed sections of Beams BG2-IV-E4 and BG2-IV-E1, respectively. These figures show that both beams failed by rupture in the strengthening sheets, followed by yielding in steel bars and fracture of the beams in a V-shape. Therefore, the use of epoxy Type 1 or 4 enabled the sheets to reach their full strength with no delamination.

The failed sections of Beams CP1-V, CP2-V, and CP3-V are shown in Fig. 8(k), (l), and (m), respectively. The cracking patterns of beams CP1-V, CP2-V, and CP3-V indicate that the bonding of CFRP plates on the sides of the beams resulted in fewer and wider cracks along the beam lengths. In addition, the presence of CFRP plates on the sides of the beams did not change the angle of inclination of the cracks, since these plates carried stresses only in their longitudinal direction and did not carry any shear force. The three beams failed in a tension, with a horizontal shear failure in the concrete near CFRP plates. No delamination or rupture of fibers was noted in the three tested beams. Therefore, epoxy Type 4, coupled with the CFRP plates, was stronger than the concrete. In addition, the shear failure in the concrete is attributed to stress concentration near the CFRP plates.

Ductility

The ductility of a beam can be defined as its ability to sustain inelastic deformation without loss in load carrying capacity, prior to failure. Ductility can be defined in terms of deformation or energy. In the case of steel-reinforced beams, where there is clear plastic deformation of steel at yield, ductility can be calculated using deformation methods. It can be defined as the ratio of ultimate deformation to the deformation at yield. The deformations can be strains, deflections, or curvatures. In the case of beams strengthened with FRP, there is usually no clear yield point; therefore, the classical definition of ductility cannot be applied. In addition, due to the low modulus of elasticity of the FRP materials, the FRP-strengthened beams usually experience large deformations. These large deformations do not mean ductile behavior. Therefore, based on the energy definition, ductility may be expressed by a ratio relating any two of the inelastic, elastic, and total energies. For comparison, the ratio of the inelastic energy to the total energy is considered to be the energy ratio. The total energy is the area under the load-deformation curve, which can be easily calculated. The problem that remains is how to separate the elastic energy from the inelastic energy. A proposed approach[9] is shown in Fig. 9. Detailed discussion of this approach can be found elsewhere.[9]

The slope of the line separating the elastic energy and the inelastic energy is

$$S = \alpha\beta\gamma\frac{E_f}{E_s} \times \frac{f_y}{f_{ds}}\frac{P_1S_1 + (P_2 - P_1)S_2 + (P_3 - P_2)S_3}{P_3} \qquad (1)$$

where

P_1, P_2, and P_3 are loads shown in Fig. 9, and S_1, S_2, and S_3 are the corresponding slopes.

α = constant depends on type of shear reinforcement (vertical external reinforcement);
β = constant depends on type of flexural reinforcement (longitudinal external reinforcement);
γ = constant depends on the mode of failure (equals to 1 in case of flexural failure);
E_f = modulus of elasticity of FRP laminates;
E_s = modulus of elasticity of steel;
f_y = yield strength of steel; and
f_{ds} = design failure strength of FRP, usually 60 percent of

Table 6—Energy ratios of tested beams

Group	Beam designation	Energy ratio*	Failure mode
1	CF-I	(0.61)†	Rupture of FRP sheets
	CFS-I	(0.63)†	
2	CFS-II	0.61	
	UG1-III	0.58	
	UG2-III	0.64	Concrete crushing
3	BG1-IV	0.67	Rupture of FRP sheets
	BG2-IV‡	0.73	Bond failure between resin and concrete
	BG3-IV‡	0.67	
4	BG2-IV-E4	0.64	Rupture of FRP sheets
	BG2-IV-E1	0.61	
5	CP1-V	0.68	Horizontal shear failure in concrete
	CP2-V	0.64	
	CP3-V	0.69	
CONT		0.81	Tensile failure of steel

*Ratio of inelastic energy to total energy at failure.
†Numbers between bracket not verified experimentally as these two beams were not unloaded and reloaded before failure.
‡These two beams may be excluded due to epoxy bond failure.

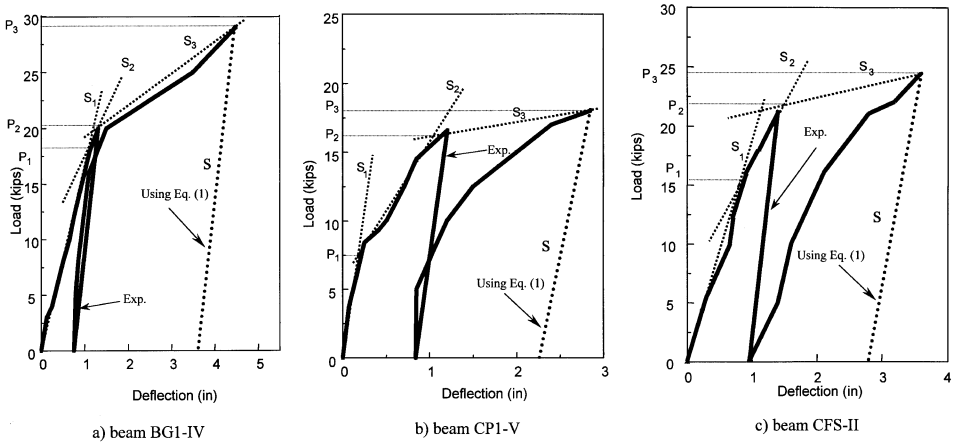

a) beam BG1-IV b) beam CP1-V c) beam CFS-II

Fig. 9—Comparison between theoretical and experimental unloading slopes: (a) Beam BG1-IV; (b) Beam CP1-V; and (c) Beam CFS-II.

maximum strength.

From the experimental results, the constants α, ß, and γ were determined as follows:

α = 1 for no shear strengthening;
α = 0.35 for shear strengthening using bidirectional GFRP sheets of strengthening System IV;
α = 0.45 for shear strengthening using unidirectional GFRP sheets of strengthening System III;
α = 0.5 for shear strengthening using CFRP sheets of strengthening Systems I and II;
β = 1 for no flexural strengthening;
β = 7.0 for flexural strengthening using bidirectional GFRP sheets of System IV;
β = 5.5 for flexural strengthening using unidirectional GFRP sheets of System III; and
β = 3.5 for flexural strengthening using System I or V.

Once the slope is determined from Eq. (1), the energy ratio can be calculated. The load-deflection relationships of three beams shown in Fig. 9 were not used in the derivation of the constants α, β, and γ. These relationships were reserved for verification of Eq. (1). The energy ratios of Beams BG2-IV-E1, CP1-V, and CFS-II are shown in Fig. 9(a) through (c), respectively. In Fig. 9, the calculated slope correlates well with the observed unloading path of the three beams.

The energy ratios of the tested beams are tabulated in Table 6. Ratios of Beams BG2-IV and BG3-IV should be excluded because these beams delaminated at maximum load. With the exception of the control beam, all of the beams exhibited poor ductility. Failures in all strengthened beams were sudden and accompanied by the release of large amounts of energy. Therefore, a reasonable factor of safety should be used in the design of FRP strengthened reinforced concrete members.

CONCLUSIONS

Based on the experimental results discussed in this paper, the following can be concluded:

1. The use of FRP laminates in strengthening concrete beams reduces deflections and increases load carrying capacity in the beams. Cracks that do occur are smaller and more evenly distributed. Furthermore, the use of FRP vertical layers can help to further reduce deflections and to further increase ultimate load carrying capacity. The presence of vertical layers also prevents rupture in the flexural (horizontal) strengthening fibers.

2. The ultimate load carrying capacity of beams can be doubled by using a proper combination of horizontal and vertical fibers coupled with the proper epoxy.

3. Extending the vertical layers over the entire span of the beam reduces the diagonal cracks so that the longitudinal fibers are fully used and the load carrying capacity of the beams is significantly increased.

4. The use of CFRP plates on the bottom and sides of the beam improves the response in comparison with using CFRP plates only at the bottom of the beam.

5. All the FRP strengthened beams exhibited brittle behavior requiring a higher factor of safety in design.

REFERENCES

1. ACI Committee 440, "State-of-the-Art Report on Fiber-Reinforced Plastic (FRP) Reinforcement for Concrete Structures (ACI 440R-96)," American Concrete Institute, Farmington Hills, Mich., 1996, 65 pp.

2. Saadatmanesh, H., and Ehsani, M. R., "RC Beams Strengthened with GFRP Plates," Parts I and II, *Journal of Structural Engineering*, ASCE, V. 117, No. 11, 1991, pp. 3417-3455.

3. Alfarabi, S.; Al-Sulaimani, G.; Basunbul, I.; Baluch, M.; and Ghaleb, B., "Strengthening of Initially Loaded Reinforced Concrete Beams Using FRP Plates," *ACI Structural Journal*, V. 91, No. 2, Mar.-Apr. 1994, pp. 160-169.

4. Alfarabi, S.; Al-Sulaimani, G.; Basunbul, I.; Baluch, M.; and Ghaleb, B., "Shear Repair for Reinforced Concrete by Fiberglass Plate Bonding," *ACI Structural Journal*, V. 91, No. 3, May-June 1994, pp. 458-465.

5. Malek, A. M.; Saadatmanesh, H.; and Ehsani, M., "Prediction of Failure Load of Reinforced Concrete Beams Strengthened with FRP Plate Due to Stress Concentration at Plate Ends," *ACI Structural Journal*, V. 95, No. 1, Jan.-Feb. 1998, pp. 142-152.

6. He, J. H.; Pilakoutas, K.; and Waldron, P., "Strengthening of Reinforced Concrete Beams with CFRP Plates," *Proceedings of the Third International Symposium on Nonmetallic (FRP) Reinforcement for Concrete Structures*, Sapporo, Japan, 1997, pp. 343-350.

7. Takahashi, Y.; Sato, Y.; Ueda, T.; Maeda, T.; and Kobayashi, A., "Flexural Behavior of RC Beams with Externally Bonded Carbon Fiber Sheet," *Proceedings of the Third International Symposium on Nonmetallic (FRP) Reinforcement for Concrete Structures*, Sapporo, Japan, 1997, pp. 327-334.

8. Swamy, N.; Mukhopadhyaya, P.; and Lynsdale, C., "Ductility Consideration in Using GFRP Sheets to Strengthen and Upgrade Structures," *Proceedings of the Third International Symposium on Nonmetallic (FRP) Reinforcement for Concrete Structures*, Sapporo, Japan, 1997, pp. 637-644.

9. Grace, N. F.; Soliman, A. K.; Sayed, G. A.; and Saleh, K. R., "Behavior and Ductility of Simple and Continuous Beams Reinforced with FRP Bars and Stirrups," accepted for publication, ASCE *Journal of Composites for Construction*, Nov. 1998.